Available online at www.sciencedirect.com
ScienceDirect
Trans. Nonferrous Met. Soc. China 21(2011) 330−334
Transactions of Nonferrous Metals Society of China
www.tnmsc.cn

Effects of heat treatment temperature on oxidation behavior of glass-like carbon derived from acetone-furfural resin

XIA Lun-gang, ZHANG Hong-bo, XIONG Xiang

State Key Laboratory for Powder Metallurgy, Central South University, Changsha 410083, China

Received 1 February 2010; accepted 29 November 2010

Abstract: Glass-like carbons (GCs) were prepared by carbonization of acetone-furfural resin in nitrogen atmosphere at 850 °C, followed by heat treatment over a range of 1 200−2 500 °C in inert atmosphere. The effect of heat treatment temperature (HTT) on the oxidation behavior was investigated by dynamic and isothermal thermogravimetric analyses. The structure of GC was examined by X-ray diffractometry (XRD) and the morphologies of GC before and after oxidation were examined by scanning electron microscopy (SEM). It is shown that the GC samples present peculiar oxidation behavior. The anti-oxidation behavior increases with increasing the HTT to 1 600 °C, whereas decreases gradually thereafter. GC sample heat treated at 1 600 °C obtains relatively optimal anti-oxidation properties under this condition. During the oxidation, this material produces grid network matrix surface and numerous nodular residues on the surface, resulting in excellent resistance to the attack of oxygen atoms.
Key words: glass-like carbon; acetone-furfural; kinetics; heat treatment temperature; microstructure

1 Introduction

Since its initial preparation, glass-like carbon (GC) has received considerable attention in a wide spectrum of areas, ranging from battery to semiconductor industries, because of its remarkable characteristics, such as great hardness and gas impermeability[1−3]. GC is often produced by pyrolysis of organic polymeric precursors, such as polyfurfuryl alcohol, acetone-furfural, phenol-formaldehyde, or polyvinyl chloride, either in the inert or in a vacuum atmosphere in order to avoid combustion of the precursors[4−5]. Due to its significant influence on the applications, the oxidation behavior of GC, mainly derived from polyfurfuryl alcohol and phenol-formaldehyde, has been extensively investigated. Several groups revealed that the effects of molecular oxygen are on the external surface and produce minor changes on the porosity[6−7]. Most of the work reported indicated that upon oxidation the apparent activation energy generally increases with increasing the heat treatment temperature (HTT), and the anti-oxidation properties are improved by the higher HTT[8−11].

In this work, thermogravimetric analyses (TGA) were applied to investigating the dynamic and isothermal oxidation behavior of acetone-furfural-derived GC in order to evaluate the effects of HTT on the anti-oxidation properties. The structure of GC and the morphologies of GC before and after oxidation were examined. A peculiar oxidation behavior was found, which is not observed in those derived from polyfurfuryl alcohol and phenolic resin and is not reported by other researchers so far, to our knowledge. The reaction kinetics and oxidation mechanisms were also analyzed.

2 Experimental

The GC samples were made from commercially available acetone-furfural resin. The precursor resin was homogeneously admixed with 7 % phosphorous acid as hardening agent by an ultrasonication apparatus. After that, the mixture was cured at 90 °C for 24 h, then at 200 °C for 1 h in the end in an evacuated desiccator to facilitate the release of volatile products. Then the GC samples were obtained by carbonizing the cured samples at 850 °C for 1 h in nitrogen atmosphere with a very low heating rate. Subsequently, the GC samples underwent HTT of 1 200, 1 600, 2 000, 2 300, and 2 500 °C for 1 h in inert atmosphere and were denoted as GC850, GC1200, GC1600, GC2000, GC2300, and GC2500,

Foundation item: Project (2006CB600902) supported by the National Basic Research Program of China
Corresponding author: ZHANG Hong-bo; Tel: +86-731-88877393; E-mail: xialung@live.cn
DOI: 10.1016/S1003-6326(11)60717-6

respectively. They were machined to obtain specimens of dimensions 2 mm×2 mm×1 mm for following oxidation.

The oxidation properties were measured by dynamic and isothermal scans using a SDTQ600 thermogravimetric analyzer. The dynamic oxidation scans were performed under dry air flow of 100 mL/min, with a heating rate of 10 °C/min until its total combustion. The thermogravimetric (TG) and differential scanning calorimetric (DSC) curves were obtained. The isothermal scans were conducted at 1 000 °C for 30 min. The GC samples were heated from room temperature to 1 000 °C under nitrogen flow. When the given temperature was reached, the N_2 flow was changed to dry air flow with a 100 mL/min rate. The TG curve was obtained and the differential thermogravimetric (DTG) curve was obtained in terms of TG data.

The X-ray diffraction (XRD) patterns of GC samples were recorded by using Rigaku D/max2550VB X-ray diffractometer with silicon powder as the inner standard. The samples were analyzed by Cu K_α radiation (λ=1.540 6 Å) produced at 40 kV and 200 mA. When the obtained profiles appeared to overlap, they were separated with a Pearson VII type function. The average interplanar spacing d_{002} and crystallite size L_c were calculated from the Bragg formula and the Scherrer formula, respectively. The bulk density and apparent porosity were determined by Archimedes' method. The morphologies of GC samples before and after oxidation were analyzed by scanning electron microscope (SEM, Nova NanoSEM 230).

3 Results and discussion

3.1 X-ray diffraction

Powder X-ray diffraction patterns were collected for each GC sample and are depicted in Fig.1. The profiles from (002) plane at about 26° are shown with silicon powder as the inner standard at about 28.5°. It is apparent that the GC samples with HTT lower than 2 300 °C have quite weak (002) peaks, which is indicative of a high degree of disorder in the graphemes. When the HTT is as high as 2 500 °C, the (002) peak is shifted toward 26.5°, characterizing crystalline graphite. But it is still weak and asymmetrical, indicating that the carbon still presents typical amorphous structure. The structural parameters calculated by the Bragg formula and Scherrer formula[12] are summarized in Table 1. Because of the absence of distinguishable peaks from those with HTT lower than 2 300 °C, the structural parameters cannot be convincingly obtained in this instance. From Table 1, it is shown that the GC2500 has a d_{002} of 3.46 Å and an L_c of 43 Å, suggesting that the turbostratic component is formed in this carbon structure. However, it is a fairly low stage of crystallinity and no graphitization conversion takes place until this HTT[13]. Significant stacking of the layer planes does not occur; neither does edge coalescence. So the GCs must be considered globally amorphous.

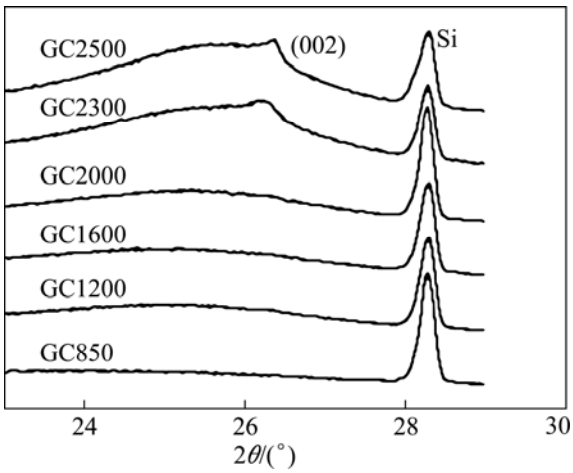

Fig.1 X-ray diffraction patterns of GC samples

Table 1 Structural parameters of GC samples

HTT/°C	d_{002}/Å	L_c/Å
2 300	3.48	43
2 500	3.46	43

3.2 Density and porosity

Moreover, the bulk density and apparent porosity of GC samples were tested by Archimedes' method as shown in Fig.2. The results indicate that, the bulk densities of GCs from acetone-furfural resin and those from polyfurfuryl alcohol and phenolic resin[2] have a similar tendency in the change. In contrast, the apparent porosities obtained in this study are much larger (from 2.0% to 5.2% with increase of HTT from 850 °C to 2 500 °C). It can be attributed to the difference of precursors used, namely, the difference of cross-linking

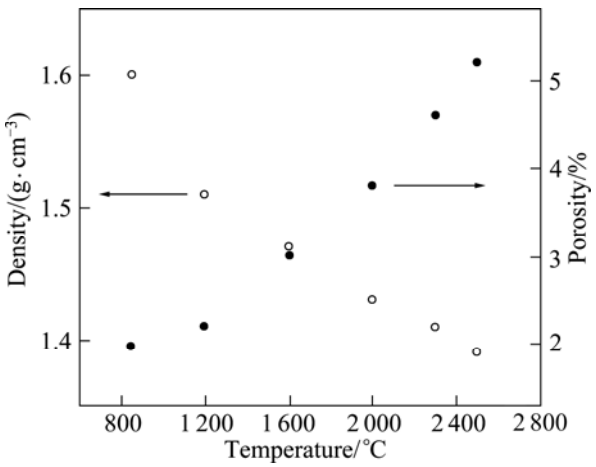

Fig.2 Bulk density and apparent porosity of GC samples

of molecules, which is considered to affect the resultant carbon structure. On the other hand, the carbonizing process is involved, which is considered to affect the escape of volatile products during the carbonization. With the development of apparent porosity, more edge-planes and disordered carbon atoms appear on the walls of pores, which facilitates the attack of oxygen atoms[7, 14−15].

3.3 Oxidation properties

The results of dynamic and isothermal measurements are displayed in Fig.3. From the TG and DSC curves of dynamic scans (Figs.3(a) and (b)), it is interesting to note that the oxidation reaction temperatures (t_i, t_m and t_f) increase with the increase of HTT up to 1 600 °C, whereas decrease gradually after this temperature. Upon oxidation at 1 000 °C for 30 min, the oxidation mass loss (TG) and oxidation rate (DTG) of GC1600 are both the least (Figs. 3(c) and (d)), with only 14.6% of mass loss, indicating that this HTT invests GC relatively optimal anti-oxidation properties under this condition.

The apparent activation energy (E_a) of dynamic oxidation was calculated from the Arrhenius plot (Fig.4) and presented in Table 2 (calculated according to Ref.[16]). From the different values of E_a for one sample, it can be concluded that there are different oxidation mechanisms and oxidation kinetics with increasing oxidation temperature. Based on the data in Table 2, it is evident that for GC850 and GC1200 two oxidation mechanisms appear with increasing the oxidation temperature; for GC1600 and GC2000 one mechanism appears; and for GC2300 and GC2500 two mechanisms appear again. It can be inferred that the oxidation mechanism changes from surface reaction controlled at lower oxidation temperatures and diffusion controlled at higher oxidation temperatures to diffusion controlled merely during the whole oxidation process, then to diffusion controlled at lower temperatures and surface reaction controlled at higher temperatures, with increasing the HTT. The E_a value of GC1600 is the maximal among all samples, confirming that this GC

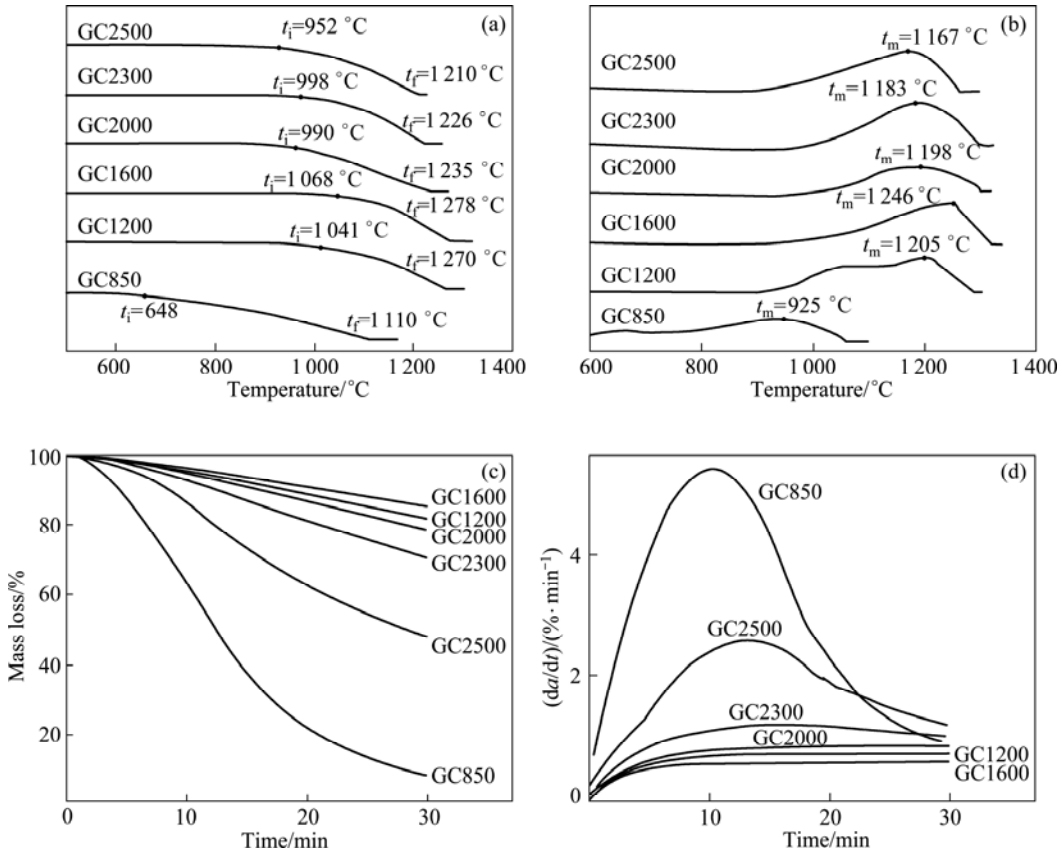

Fig.3 Oxidation properties of GCs: (a) TG and (b) DSC curves of dynamic scans; (c) TG and (d) DTG curves of isothermal scans (t_i: Beginning temperature of GC oxidation; t_m: Maximum temperature of oxidation velocity; t_f: Complete oxidation temperature of GC)

Table 2 Apparent activation energy of dynamic oxidation

HTT/°C	850	1 200	1 600	2 000	2 300	2 500
E_{a1}/(kJ·mol^{-1})	142.3	208.4	221.3	188.5	161.4	167.3
E_{a2}/(kJ·mol^{-1})	74.4	184.6	221.3	188.5	158.9	140.7

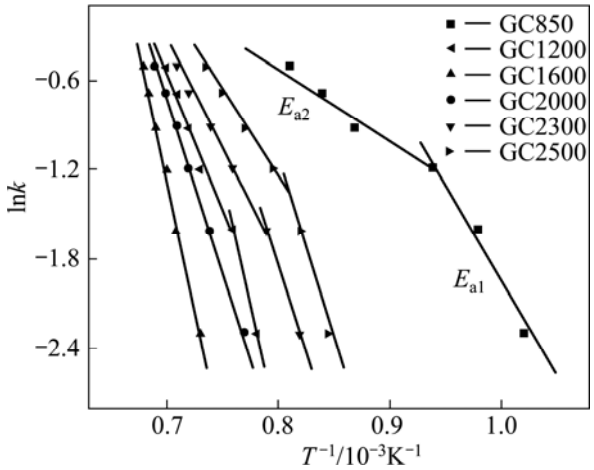

Fig.4 Arrhenius plots of oxidation rates for GC samples at different heat treatment temperatures

sample obtains relatively optimal anti-oxidation properties under this condition. This result differs from previous results, concluding that the higher the HTT, the better the anti-oxidation of the glass-like carbon[9–11].

3.4 Oxidized morphology and oxidation mechanism

Fig.5 shows the typical surface morphologies of GC samples before and after oxidation. Because of their high luster and glass-like fracture characteristics, the GC samples with different HTTs have similar morphology under SEM technique. As a consequence, a typical image with no oxidation for GC2000 and typical oxidized surfaces of GC samples are given in Fig.5. It can be seen that, there are semispherical grains attached to the oxidized surface of GC850, and on the oxidized surface of GC1600 there are numerous nodular residues, while on the oxidized surface of GC2000 there are a large amount of small spherical grains attached to the residual carbon matrix. Based on the differences of surface morphologies, we can deduce that in spite of similar composition and crystallinity, it is more difficult for the attack of oxygen atoms to proceed on the surface with nodular grains due to tight junction with matrix, than on the surfaces with semispherical and spherical grains. It can be considered to be the main factor leading to the excellent anti-oxidation property of GC1600 under this condition.

From the results of XRD and apparent porosity measurements for the GCs derived from acetone-furfural resin, it is observed that crystalline size and porosity grow and the interlayer space narrows with increasing HTT. Upon oxidation, the microstructure of GCs and open pores simultaneously affect the anti-oxidation property. Because of the similar closed and nanoporous characteristics, the apparent porosity of GC has no

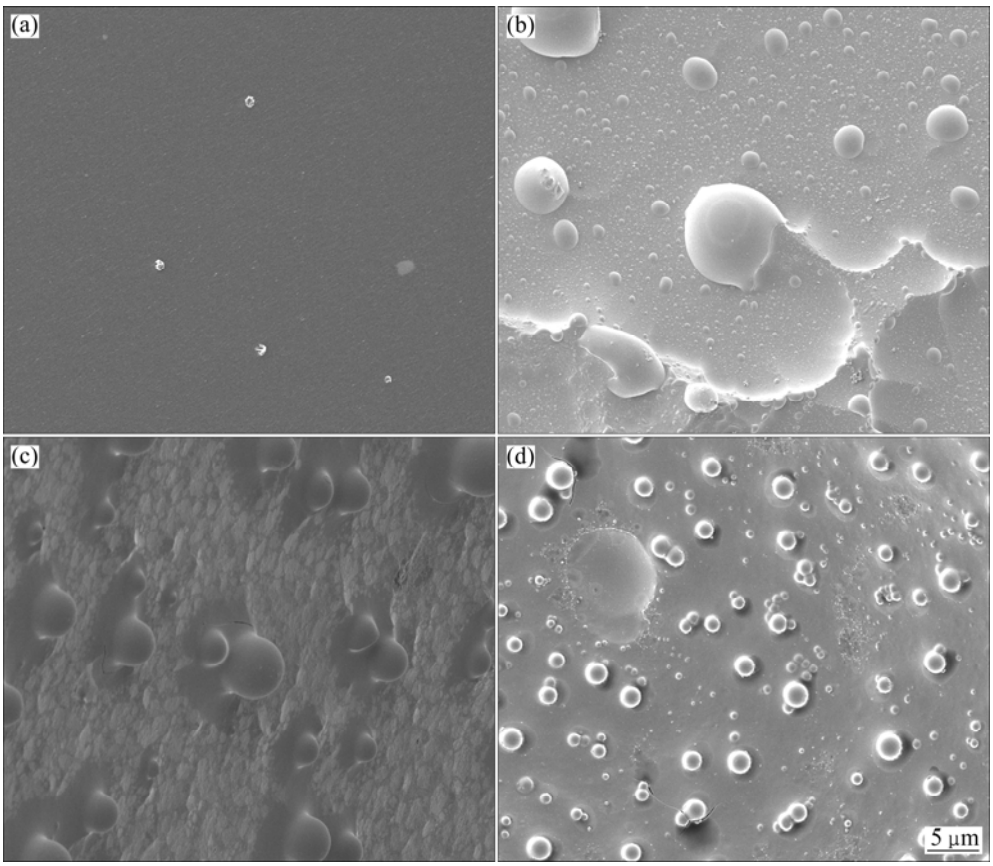

Fig.5 SEM images of no oxidation for GC2000 (a), and oxidized surfaces of GC850 (b), GC1600 (c) and GC2000 (d)

essential effect on the oxidation properties of GCs with different HTTs when the oxidation process proceeds to a certain extent. It can be speculated that the GC with multi-component structure of amorphous and graphite-like carbons has excellent anti-oxidation property.

4 Conclusions

1) GC derived from acetone-furfural resin shows peculiar oxidation behavior with increasing the HTT, compared with that derived from polyfurfuryl alcohol and phenolic resin under similar conditions.

2) GC heat treated at 1 600 °C obtains relatively optimal anti-oxidation property. The anti-oxidation property is attributed to the different microstructures of GC.

3) Upon the oxidation, GC1600 produces grid network matrix surface and numerous nodular residues on the surface, resulting in excellent resistance to the attack of oxygen atoms. However, additional experiments are required to provide a more comprehensive understanding of the generation of this structure and its anti-oxidation mechanism.

References

[1] YAMADA S, SATO H. Some physical properties of glassy carbon [J]. Nature, 1962, 193(20): 261−262.

[2] FIZER E, SCHAEFER W. The effect of cross-linking on the formation of glasslike carbon from thermosetting resin [J]. Carbon, 1970, 8(3): 353−364.

[3] PESIN L A. Review: Structure and properties of glass-like carbon [J]. Journal of Materials Science, 2002, 37(1): 1−28.

[4] SCHUELLER O J A. Preparation and characterization of doped glassy carbon materials application to fuel cell electrodes [D]. Columbus: Ohio State Univ, 1995.

[5] SCHUELLER O J A, BRITTAIN S T, WHITESIDES G M. Fabrication of glassy carbon microstructures by pyrolysis of microfabricated polymeric precursors [J]. Advanced Materials, 1997, 9(6): 477−480.

[6] DOMINGO-GARCIA M, LÓPEZ-GARZÓN F J, PÉREZ-MENDOZA M. Modifications produced by O_2 plasma treatments on a mesoporous glassy carbon [J]. Carbon, 2000, 38(4): 555−563.

[7] BRAUN A, BÄRTSCH M, SCHNYDER B, KÖTZ R, HAAS O, WOKAUN A. Evolution of BET internal surface area in glassy carbon powder during thermal oxidation [J]. Carbon, 2002, 40(3): 375−382.

[8] TANABE Y, UTSUNOMIYA M, ISHIBASHI M, KYOTANI T, KABURAGI Y, YASUDA E. Oxidation behavior of furfural-acetone-resin-derived carbon alloyed with Ta or Ti [J]. Carbon, 2002, 40(11): 1949−1955.

[9] RODRIGUEZ-REINOSO F, Jr WALKER P L. Reaction of glassy carbon with oxygen [J]. Carbon, 1975, 13(1): 7−10.

[10] LI Jun, LUO Rui-ying, LIN Chen, BI Yan-hong, XIANG Qiao. Oxidation resistance of a gradient self-healing coating for carbon/carbon composites [J]. Carbon, 2007, 45(13): 2471−2478.

[11] NAKAMURA K, TANABEB Y, FUKUSHIMAC M, TERANISHID Y, AKATSUE T, YASUDAE E. Analysis of surface oxidation behavior at 500 °C under dry air of glass-like carbon heat-treated from 1200 to 3000 °C [J]. Materials Science and Engineering B, 2009, 161(1−3): 40−45.

[12] YANG Xin, HUANG Qi-zhong, ZOU Yan-hong, CHANG Xin, SU Zhe-an, ZHANG Ming-yu, XIE Zhi-yong. Anti-oxidation behavior of chemical vapor reaction SiC coatings on different carbon materials at high temperatures [J]. Trans Nonferrous Met Soc China, 2009, 19(5): 1044−1050.

[13] BURKET C L, RAJAGOPALAN R, FOLEY H C. Overcoming the barrier to graphitization in a polymer-derived nanoporous carbon [J]. Carbon, 2008, 46(3): 501−510.

[14] BURKET C L, RAJAGOPALAN R, MARENCIC A P, DRONVAJJALA K, FOLEY H C. Genesis of porosity in polyfurfuryl alcohol derived nanoporous carbon [J]. Carbon, 2006, 44(14): 2957−2963.

[15] GAO Peng-zhao, BAI Yong-mei, LIN Sen, GUO Wei-ming, XIAO Han-ning. Microstructure and non-isothermal oxidation mechanism of biomorphic carbon template [J]. Ceramics International, 2008, 34(8): 1975−1981.

[16] BOKOVAA M N, DECARNEA C, ABI-AADA E, PRYAKHINB A N, LUNINB V V, ABOUKAÏSAB A. Kinetics of catalytic carbon black oxidation [J]. Thermochimica Acta, 2005, 428(1−2): 165−171.

热处理温度对糠酮树脂基玻璃炭氧化性能的影响

夏伦刚，张红波，熊 翔

中南大学 粉末冶金国家重点实验室，长沙 410083

摘 要：选用糠酮树脂为前驱体，在氮气保护气氛下经 850 °C 炭化制备出玻璃炭样品，随后在 1 200~2 500 °C 温度范围内对样品进行高温热处理。采用动态热分析和等温热分析两种方法研究热处理温度对糠酮树脂基玻璃炭氧化性能的影响规律。采用 X 射线衍射（XRD）和扫描电镜(SEM)分别分析样品的晶体结构和表面形貌。结果表明：糠酮树脂基玻璃炭的氧化行为较为特别，随着热处理温度的升高，样品的抗氧化性能增强，但当热处理温度超过 1 600 °C 后，抗氧化性能开始下降，1 600 °C 热处理后的样品的抗氧化性能最佳。该样品在氧化过程中表面形成网格状的基体和许多瘤节状残留物，这种特殊的氧化形貌有利于增强样品的抗氧化性能。

关键词： 玻璃炭; 糠酮树脂；动力学; 热处理温度; 微观结构

(Edited by LI Xiang-qun)